

Article

Optimal Spatial Coherence of a Light-Emitting Diode in a Digital Holographic Display

Sungjin Lim, Hosung Jeon, Sunggyun Ahn and Joonku Hahn *

School of Electronic and Electrical Engineering, Kyungpook National University, 80 Daehak-ro, Buk-gu, Daegu 41566, Korea; dlatjdwls0326@knu.ac.kr (S.L.); jhs0485@knu.ac.kr (H.J.); geni4160@knu.ac.kr (S.A.)

* Correspondence: jhahn@knu.ac.kr

Abstract: The coherence of a light source is a vital aspect regarding the image quality of holographic contents. Generally, the coherence of the light source is the reason for speckle noise in a holographic display, which degrades the image quality. To reduce the speckle noise, partially coherent light sources such as light-emitting diodes (LED) have been studied. However, if the coherence of the light source is too low, the reconstructed image will blur. Therefore, using a spatial filter to improve the spatial coherence of LEDs has been proposed. In this study, we analyze the effect of the spatial and temporal coherence of the LED light source in a digital holographic display, and the optimal spatial coherence is determined. For this purpose, we devised an optical structure to control the spatial coherence in a holographic display system using a digital micro-mirror device (DMD). Here, the DMD functions as a dynamic spatial filter. By evaluating the change in the holographic image quality according to the spatial filter size, we obtained an optimal spatial filter size of 270 μm in our system. The proposed method is expected to be useful for selecting the optimal coherence of the light source for holographic displays.

Keywords: digital holographic display; coherence system; digital micro-mirror device; light-emitting diode



Citation: Lim, S.; Jeon, H.; Ahn, S.; Hahn, J. Optimal Spatial Coherence of a Light-Emitting Diode in a Digital Holographic Display. *Appl. Sci.* **2022**, *12*, 4176. <https://doi.org/10.3390/app12094176>

Academic Editors: Ting-Chung Poon, Hiroshi Yoshikawa, Yaping Zhang, Liangcai Cao and Taegeun Kim

Received: 22 March 2022

Accepted: 18 April 2022

Published: 21 April 2022

Publisher's Note: MDPI stays neutral with regard to jurisdictional claims in published maps and institutional affiliations.



Copyright: © 2022 by the authors. Licensee MDPI, Basel, Switzerland. This article is an open access article distributed under the terms and conditions of the Creative Commons Attribution (CC BY) license (<https://creativecommons.org/licenses/by/4.0/>).

1. Introduction

Holographic displays completely generate the wavefront of contents, unlike conventional two-dimensional displays that present only the intensity information of contents [1–5]. This means that holographic displays can solve some of the problems of conventional 3D displays, such as the vergence–accommodation conflict and discontinuous motion parallax. In the optics of holographic displays, the coherence of the light source is important for reconstructing the holographic content, because holographic displays are based on the interference phenomenon of light [6–8]. However, a high coherence leads to the speckle noise which degrades the quality of holographic contents [9,10].

Various techniques for reducing speckle noise have been proposed, such as the time-averaged superposition method, phase grating, and diffusers [11–14]. The time-averaged superposition method uses a filter array of the Fourier domain or a light source array. This is constructed by synchronizing the position of the filter or the light source with a spatial light modulator, and the speckle noise is reduced by rapidly converting the hologram according to the position of the filter or the light source. The method using a diffuser is implemented by rotating the diffuser in front of a highly coherent light source, which downgrades the spatial coherence of the light source. However, these techniques cause complexity of the optics and a computational burden in holographic displays.

As another method to reduce speckle noise, holographic displays using a partially coherent light-emitting diode (LED) light source have been actively studied [15–18]. This method has clear advantage in that it can be easily implemented because the coherent light source is simply replaced by an LED. In some digital holographic displays using an LED light source, a spatial filter, (such as a pinhole), is used to set a suitable spatial coherence

from the LED light source. A spatial filter serves to limit the coherence of the light source. However, although using a partially coherent LED light source can reduce the speckle noise, it also causes a blurring of holographic contents because the LED light source has a lower coherence than a coherent light source, such as light amplification by the stimulated emission of radiation (LASER).

D. Chu et al. analyzed a reconstructed holographic image according to the coherence properties by using different light sources, such as diode-pumped solid-state lasers, LEDs, laser diodes, and super luminescent LEDs [19]. They analyzed the temporal and the spatial coherences according to light sources in relation to the speckle contrast and image sharpness of the holographic image. They proposed that a spatial filter size smaller than 300 μm is sufficient to obtain a sharp holographic image close to the hologram plane using the LED. However, they did not suggest an optimal size for the spatial filter. In addition, although expressible depth is an important characteristic in holographic displays, they did not specify the distances where holographic images can be clearly expressed relative to the spatial filter size.

In this paper, we analyzed the effect of the spatial coherence of the LED light source in a digital holographic display. To find the optimal spatial coherence of the LED light source, we proposed an optical structure to control the spatial coherence in a holographic display system using a digital micro-mirror device (DMD), which functions as a spatial filter. By analyzing the change in the holographic image according to the spatial filter size, we obtained the optimal size of the spatial filter. In addition, we reveal the relationship between the coherence properties of the LED and expressible object distances in holographic displays.

2. Control of the Spatial Coherence in a Holographic Display System

Digital holographic displays using an LED light source generally use a spatial filter to define the spatial coherence of the LED light source. Spatial coherence is closely related to the size of the light source, and a spatial filter restricts the size of the light source. Figure 1 describes the Young's interference experiment using an LED light source with a central wavelength of λ_c . Here, r_s denotes the diameter of the LED light source, and the double slit is positioned at a distance of R from the light source. The LED light source is considered as a collection of numerous point-light sources. Among them, three point-light sources, S_1 , S_2 , and S_3 , are chosen, where one is located at the center and the others are located at the ends of the LED light source. The spherical waves formed by each point light source pass through the double slit independently. Then, an interference pattern is formed by each spherical wave. If the interference patterns formed by S_1 or S_3 have an out-of-phase difference between them, the superposition of these two interference patterns is destructed. In this case, the distance between double slits becomes the coherence distance ρ_c . Thus, the slit spacing needs to be smaller than the coherence distance, ρ_c , to distinguish the interference from the LED light source. The relation between the size of the LED light source and the coherence distance is obtained by the geometric analysis as shown in Figure 1, and it is approximately determined as [20]:

$$\rho_c \simeq \frac{R\lambda_c}{r_s}. \quad (1)$$

In Equation (1), r_s denotes the diameter of the spatial filter to restrict the size of the LED light source. This implies that the spatial coherence increases as the diameter of the spatial filter decreases in the holographic display using an LED light source. However, when the coherence of the light source increases in holographic displays, speckle noise becomes severe and the quality of the reconstructed holographic content is degraded. Therefore, we devised the optical structure to control the spatial coherence in a holographic display system and it is possible to determine the optimal size of the spatial filter. Here, the spatial filter is defined by the on-state pixels of the DMD and the size of the spatial filter is controllable.

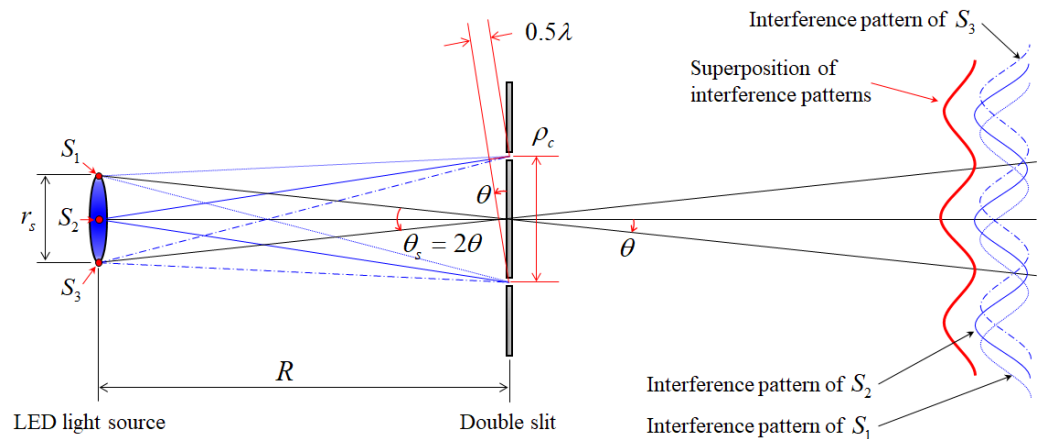


Figure 1. Relationship between the size of the light source and the spatial coherence.

Figure 2a shows the proposed holographic display system with controllable spatial coherence, which consists of an LED light source, imaging lenses, a DMD, a collimation lens, a beam splitter, an LCoS-phase-only spatial light modulator (SLM), and a Fourier lens. The LED light source has a central wavelength of 530 nm and maximum power of 20 mW. Using imaging lenses, the LED light source is imaged on the DMD. A LightCrafter with a DMD having the resolution of 608×684 pixels, manufactured by Texas Instruments, is used as a dynamic spatial filter. Here, the lateral and diagonal pitches of the pixels are 7.638 and 10.8 μm , respectively. The size of the spatial filter can be controlled by changing the on-state pixels of the DMD. The area of the on-state pixels is set to a circle and controllable as shown in Figure 2a. It is possible to increase the size of the spatial filter by 21.6 μm , and it ranges from 32.4 to 1090.8 μm . The LED light source filtered by the DMD is converted to the superposition of plane waves by the collimation lens and then it is modulated by the phase-only LCoS SLM. A collimation lens with a long focal length of 1 m is used to illuminate all active areas of the phase SLM. We used a phase-only LCoS SLM with a pixel pitch of 3.6 μm and a resolution of 3840×2160 pixels, manufactured by MAY display.

Fourier holograms are used to confirm the feasibility of the proposed system. The effect of the spatial coherence is clearly observed since the Fourier hologram transforms the optical information of the hologram to the spatial frequency domain. After the SLM is in the optical path, a Fourier lens is inserted to reconstruct the Fourier hologram with a focal length of 100 mm. The mono-color CMOS sensor has a resolution of 4096×3000 pixels, a diagonal of 1.1 inch, a pixel pitch of 3.45 μm . The experimental setup is shown in Figure 2b. In addition, because the brightness of the captured image increases with the expansion of the spatial filter size, the exposure time of the image sensor is adjusted according to the spatial filter size to prevent the saturation of the captured images, which obstructs the proposed analysis. The Lena image is used as the object of the Fourier hologram and is positioned above the DC point. Figure 3 shows the captured images of the reconstructed Fourier hologram according to the various sizes of the spatial filter with 32.4, 75.6, 140.4, 205.2, 270.0, 507.6, 702.0, and 1090.8 μm . The sharpness of the reconstructed Fourier hologram decreases and blurs as the spatial filter size increases. These results demonstrate that the reconstructed image becomes blurred owing to the decrease of the spatial coherence. It is worth noting that low temporal coherence causes radial blur, which appears clearly under a high spatial coherence.

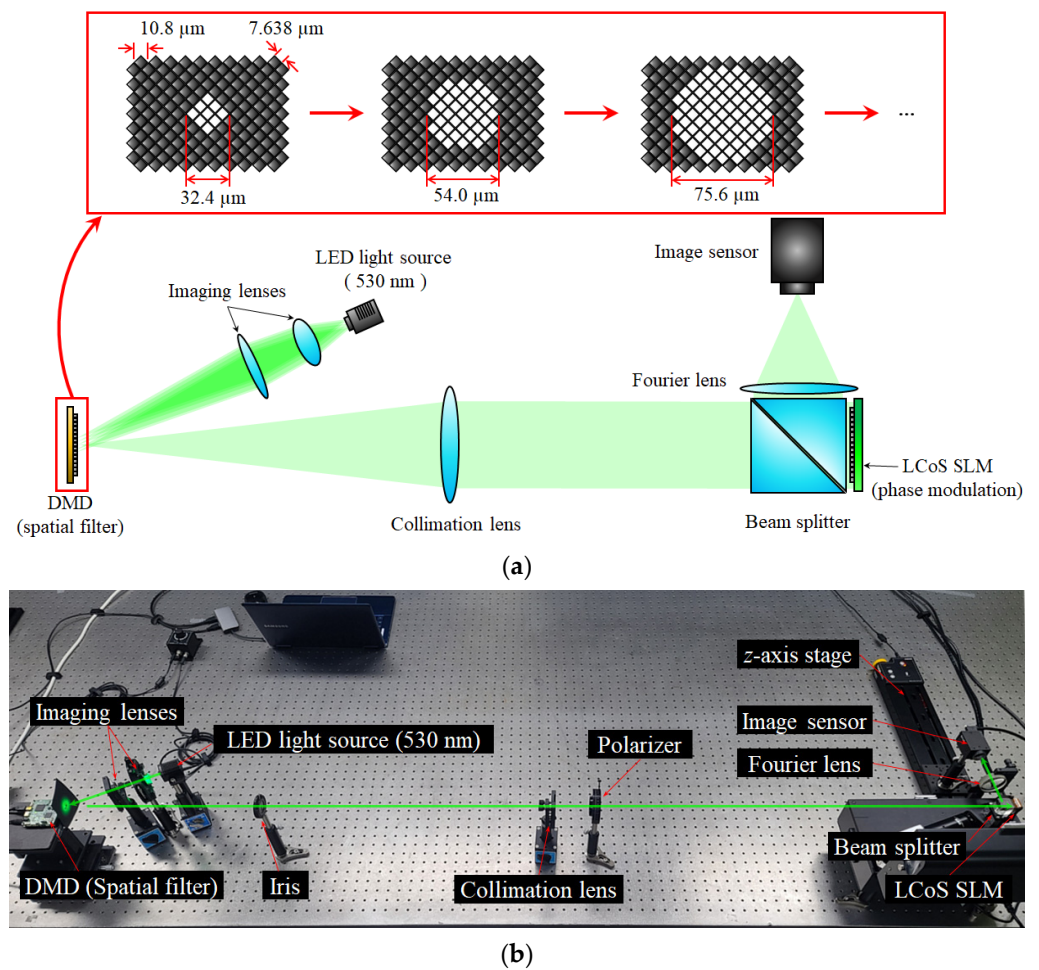


Figure 2. Holographic display system with controllable spatial coherence using a digital micro-mirror device (DMD). (a) The scheme of the proposed system and (b) the experimental setup.

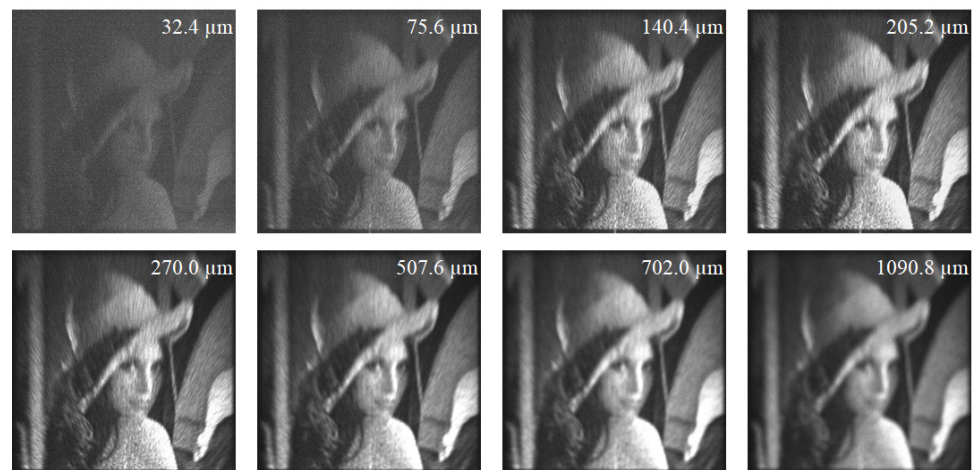


Figure 3. Reconstruction images of Fourier hologram depending on the various sizes of the spatial filter with 32.4, 75.6, 140.4, 205.2, 270.0, 507.6, 702.0, and 1090.8 μm .

3. Expressible Object Distance Range in a Hologram Depending on the Coherence

In holographic displays, the voxel reconstructed by the displays is limited by the specifications of the optics. There are some significant factors that determine the voxel size. One is the diffraction limit of the holographic display. The other is the blur caused by the coherence of the light source. Figure 4a illustrates the width of the voxel in the holographic

display, considering the spatial coherence of the LED light source. First, the width of the voxel by diffraction limit, w_{diff} , is determined as

$$w_{diff} = \frac{1.22\lambda_c|z_{obj}|}{h}, \tag{2}$$

where h and z_{obj} denote the half width of the hologram and the object distance from the hologram plane, respectively. The voxel blur owing to the spatial coherence distance is depicted in Figure 4a. If the spatial coherence is represented by the coherence distance, ρ_c , of Equation (1), the blur of the voxel owing to the coherence distance, w_{sc} , is defined by

$$w_{sc} = \frac{\lambda_c|z_{obj}|}{2\rho_c}, \tag{3}$$

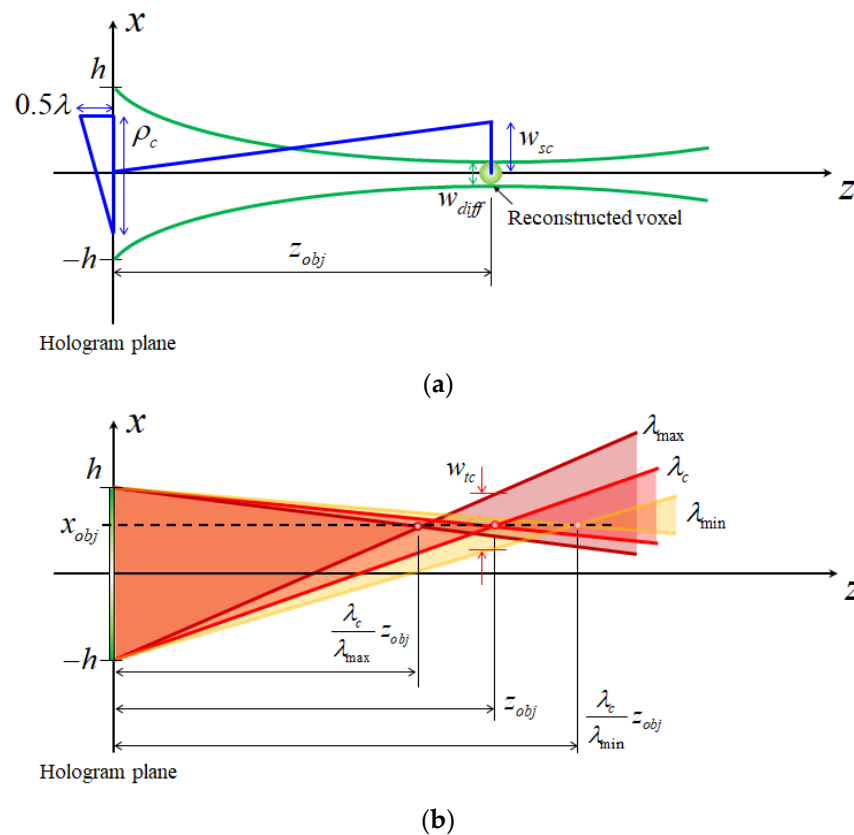


Figure 4. The effect of coherence on the size of the voxel reconstructed in the digital holographic display. (a) The width of the voxel according to both the diffraction limit and the spatial coherence and (b) the width of the voxel according to the temporal coherence.

The temporal coherence of the light source also causes the blur of the voxel and it is closely related to the full width at half maximum (FWHM) of the LED light source in the intensity distribution according to the wavelengths. In general, the FWHM of the laser light source is only several nanometers and it is reasonable for it to be considered as a delta function in display applications. However, most color LED light sources with a central wavelength of λ_c have a FWHM of several tens of nanometers. Figure 4b depicts the blur of the voxel in the holographic display when the LED light source with some amount of the spectral bandwidth is used. The blur of the voxel according to the temporal coherence is easily estimated geometrically by considering the longest and shortest wavelengths in the FWHM of the LED light source. In general, the computer-generated hologram (CGH) is generated and displayed based on the central wavelength, λ_c . When the voxel is

reconstructed at the position, z_{obj} , from the hologram plane, the position at which the voxel is reconstructed by the longest (λ_{max}) and shortest (λ_{min}) wavelengths is determined as:

$$z_{obj, \lambda_{max}} = \frac{z_{obj} \lambda_c}{\lambda_{max}}, \tag{4a}$$

$$z_{obj, \lambda_{min}} = \frac{z_{obj} \lambda_c}{\lambda_{min}}. \tag{4b}$$

Equation (4a,b) also explain the reconstructed position of the voxel depending on the wavelength. In Figure 4b, from Equation (4a,b), the blur of the voxel by the temporal coherence w_{tc} is determined as:

$$w_{tc} = \frac{(|x_{obj}| + h)(\lambda_{max} - \lambda_{min})}{\lambda_c}, \tag{5}$$

where x_{obj} is the transverse position of the voxel along the x -axis. From Equation (5), it is confirmed that the blur by the temporal coherence increases as the voxel is farther away from the optical axis and as the FWHM of the spectral bandwidth increases. Also, this indicates that the temporal coherence of the light source affects the radial blur of the voxel in the object plane. Radial blur is observed as shown in the result with a spatial filter size of 270 μm of Figure 3. Therefore, the width of the voxel, w , of the holographic display using the LED light source is the summation of the diffraction-limit width of the voxel, w_{diff} , the increment of the voxel owing to the spatial coherence, w_{sc} , and the increment of the voxel owing to the temporal coherence, w_{tc} , as:

$$w = w_{diff} + w_{sc} + w_{tc} = \frac{1.22\lambda_c |z_{obj}|}{h} + \frac{\lambda_c |z_{obj}|}{2\rho_c} + \frac{(|x_{obj}| + h)(\lambda_{max} - \lambda_{min})}{\lambda_c}. \tag{6}$$

Figure 5 shows the numerical reconstruction of voxels with different positions on object plane based on the spectral specifications of the LED light source. Here, 17 voxels with different positions in the object plane are selected and a Fresnel hologram is computed based on the central wavelength, λ_c . Considering the spectral distribution of the LED light source, the increment of the voxel owing to the temporal coherence, w_{tc} , is obtained as a weighted summation of the intensity profile of the numerical reconstruction by 1 nm wavelength intervals. Then, the voxel with both the spatial and the temporal coherence is computed as a convolution of w_{tc} and w_{sc} . In this simulation, the objects distances z_{obj} are set to 50 mm and 100 mm, and the size of the spatial filter is set to 250 μm and 1000 μm . From Figure 5, it is obvious that the width of voxel increases accordingly as the size of the spatial filter increases. Also, the width of the voxel increases accordingly as the object distance increases. The blur of the reconstructed image from a low coherence is significant when the object plane is far from the hologram plane. For example, when the size of the spatial filter is 1000 μm , the voxels located at 100 mm are too blurry. This fact gives some intuition that the holographic display has the expressible maximum object distance depending on the coherence of the LED light source.

If the observer watches the holographic contents with a distance, z_{eye} , from the hologram plane, the resolvable voxel width of the human eye, w_{eye} , is defined as

$$w_{eye} = \theta_{eye}(z_{eye} - z_{obj}), \tag{7}$$

where θ_{eye} is the resolvable angle of the human eye, $\frac{1}{60} \times \frac{\pi}{180} \text{rad}$. If the width of the reconstructed voxel, w , is equal to or smaller than the resolvable voxel width, w_{eye} , it can be considered that the holographic display is capable of expressing the voxel at a specific object distance, z_{obj} . Consequently, the expressible object distance range of the holographic display is obtained using Equations (6) and (7), and it is represented as:

$$-\frac{2h\rho_c[\lambda_c z_{eye}\theta_{eye} - (h + |x_{obj}|)(\lambda_{max} - \lambda_{min})]}{\lambda_c(2.44\lambda_c\rho_c + h\lambda_c - 2h\rho_c\theta_{eye})} \leq z_{obj} \leq \frac{2h\rho_c[\lambda_c z_{eye}\theta_{eye} - (h + |x_{obj}|)(\lambda_{max} - \lambda_{min})]}{\lambda_c(2.44\lambda_c\rho_c + h\lambda_c + 2h\rho_c\theta_{eye})}. \quad (8)$$

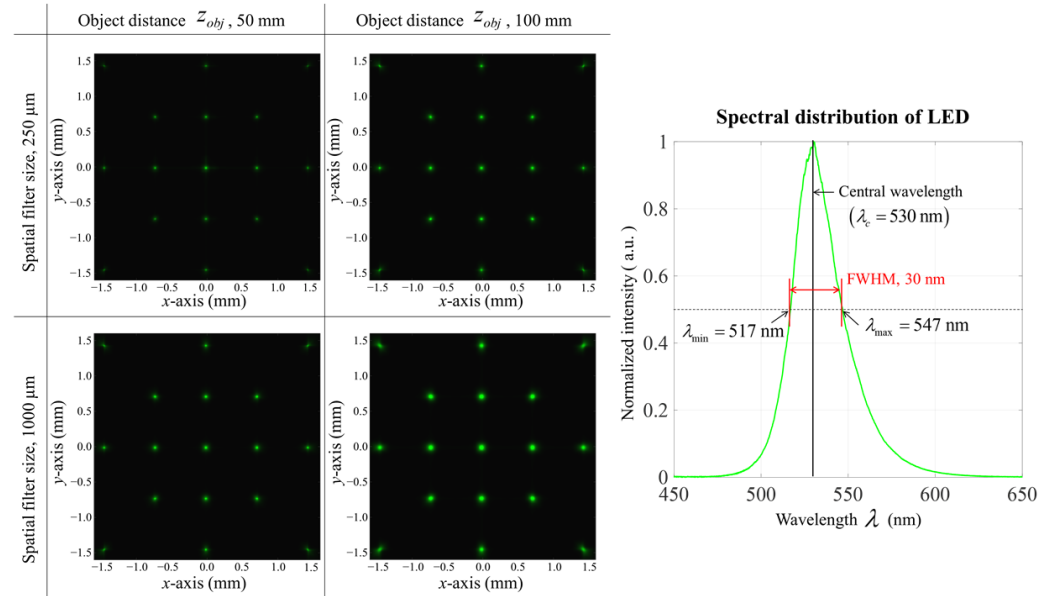


Figure 5. Numerical reconstruction of voxels with different positions on object plane and the spectral distribution of the LED light source.

Figure 6 shows the change of the expressible object distance range depending on the spatial filter size in the holographic display using an LED light source. The relationship between the expressible object distance range and the spatial filter size is represented as shown in Figure 6. In this graph, z_{eye} and h are set to 1000 mm and 3.7 mm, respectively. In Figure 6, both the red and blue areas represent the expressible object distance ranges for the voxels with different transverse positions. When the transverse position of voxel x_{obj} is 0 mm, the expressible object distance depending on the spatial filter size is the red area. When x_{obj} is 1 mm, the expressible object distance is the blue area. Naturally, the expressible object distance range narrows as the spatial filter size increases. In addition, when the voxel is placed far from the optical axis, the expressible object distance range decreases because the radial blur is dominant in the off-axis.

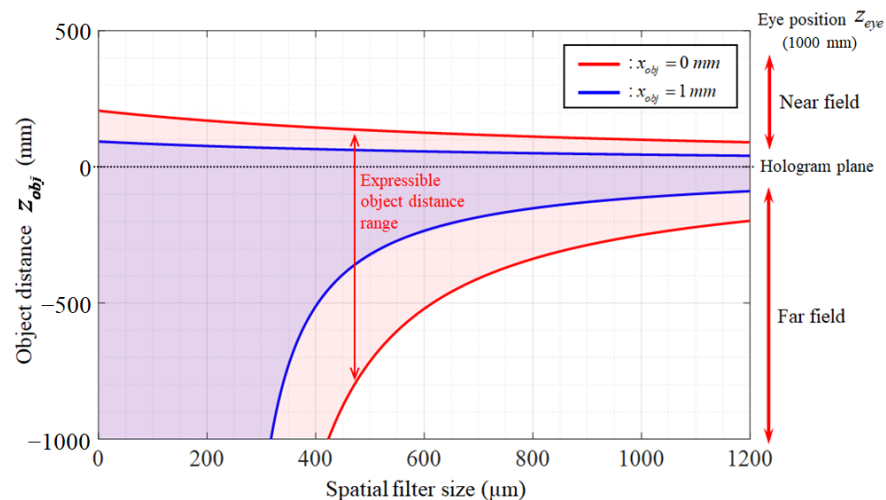


Figure 6. Expressible object distance range depending on the spatial filter size.

4. Experimental Results

To find the optimal spatial coherence of the LED in a holographic display, we performed experiments to reconstruct Fresnel holograms by changing the spatial coherence as shown in Figure 7. Figure 7a describes the optical scheme of the experiment, and the optical configuration of the experiment was equal up to that of the SLM compared to the Fourier hologram experiment described in Section 2. After the SLM in the optical path, a $4f$ optical system was inserted to remove the conjugate noise by the single-side bandpass filter. In the $4f$ optical system, the focal lengths of the two lenses were 100 mm. The experimental setup is shown in Figure 7b. Hence, the optimal size of the spatial filter was determined experimentally by measuring the image quality reconstructed by the hologram.

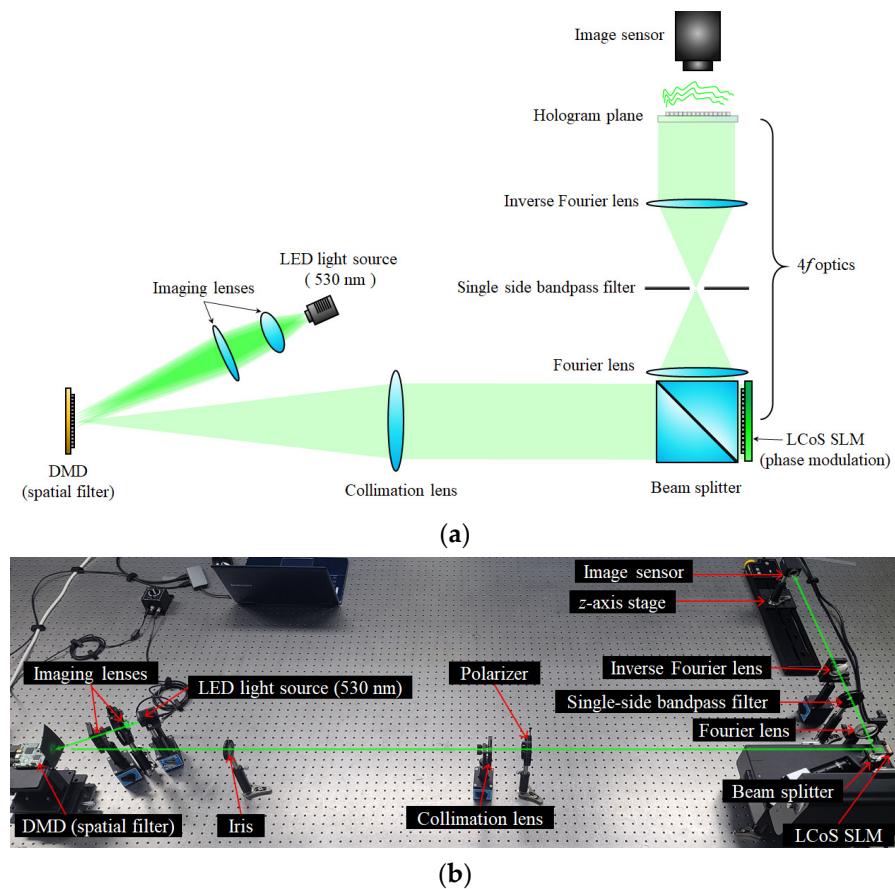


Figure 7. Experimental setup obtaining the optimal spatial coherence of the LED. (a) The optical scheme and (b) the experimental setup.

Figure 8a shows a specific target image for generating Fresnel holograms. The target object consisted of three bars to evaluate the visibility v . The average cross-section intensity distribution of the reconstructed objects was evaluated through the visibility v , given by

$$v = \frac{I_{max} - I_{min}}{I_{max} + I_{min}}, \quad (9)$$

where I_{max} and I_{min} are the central maximum intensity and neighboring minimum intensity, respectively. Visibility is a value between 0 and 1, and a value close to 1 indicates that the reconstructed image has a high sharpness. The eight target objects were located in different positions, and they were formed into two groups. Group 1 was the target object closer to the optical axis and group 2 was the target object far from the optical axis. In each group, the target objects were rotated in specific directions to check visibility in the tangential and sagittal directions. It was expected that the visibility of the tangential direction would

decrease as the target object moved farther from the optical axis owing to the temporal coherence. Fresnel holograms with a z_{obj} of 50, 100, 150, 200, and 250 mm were generated as shown in Figure 8b–f.

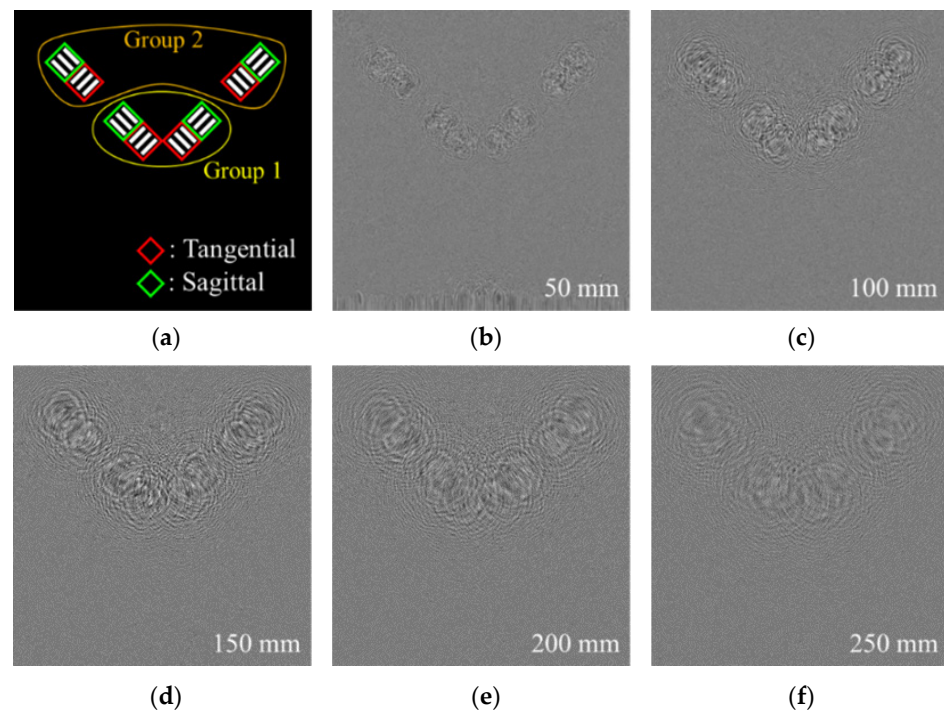


Figure 8. Fresnel holograms for experiments. (a) The target object image and Fresnel holograms of the object positioned at (b) 50, (c) 100, (d) 150, (e) 200, and (f) 250 mm from the hologram plane.

Figure 9 shows the reconstructed images for the spatial filter size of 97.2, 270.0, 507.6, 702.0, 896.4, and 1090.8 μm . The target object located at a 50 mm distance from the hologram plane was reconstructed clearly without blurring even if the spatial filter size increases. However, it was definitely confirmed that target objects in other positions were blurred as the spatial filter size increased. Moreover, the target objects farther from the hologram plane were quickly blurred as the spatial filter size increased. Among the objects of group 2, which were far from the optical axis, the tendency to blur faster than group 1 in the tangential direction was also confirmed.

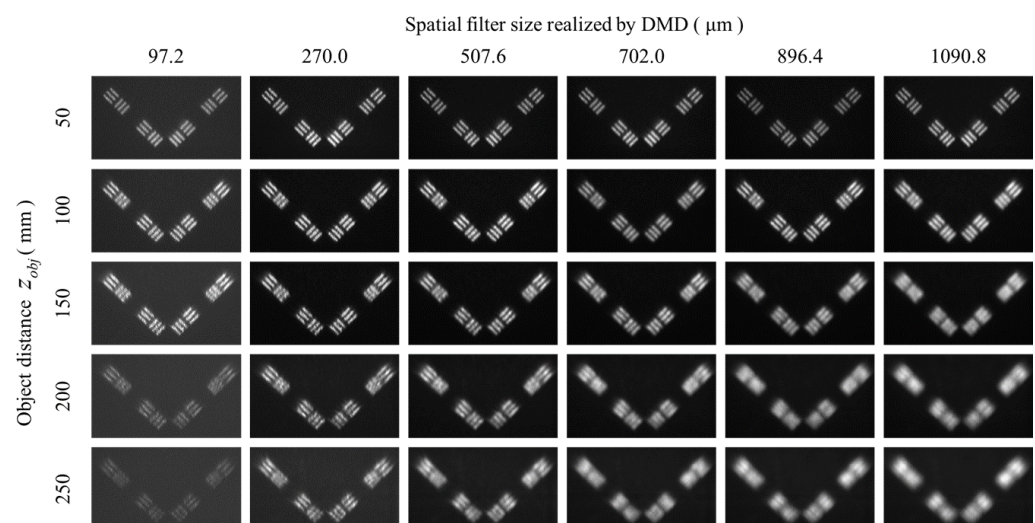


Figure 9. Reconstructed images depending on the spatial filter size of 97.2, 270.0, 507.6, 702, 896.4, and 1090.8 μm .

The change of the visibility according to the spatial filter size is shown in Figure 10. Overall, the visibility did not exceed 0.5 mainly because of speckle noise. The visibility of 0.4 was considered as the limit line because the visibility of the target object at the nearest distance, 50 mm from the hologram plane, was approximately 0.4. Visibility was expected to be improved when the spatial filter size decreased, because the expressible depth range increased when the coherence increases. This tendency was observed when the spatial filter size was larger than about 400 μm . However, visibility decreased when the spatial filter size was smaller than about 200 μm . This phenomenon can be attributed to two reasons. One is the dominance of speckle noise. As previously mentioned, an increase of the coherence results in speckle noise, and it deteriorates visibility. The other is the increase of shot noise of the CMOS sensor. The optical power passing through the spatial filter decreases significantly in proportion to its area as the size of the spatial filter decreases. In the range between 200 μm and 400 μm , the visibility did not change significantly regardless of the spatial filter size. In the tangential direction, it is obvious that the visibilities of group 2 were much lower than those of group 1. This is because a target object far from the optical axis is strongly affected by the temporal coherence. Conversely, the visibility in the sagittal direction did not change significantly, unlike in the tangential direction. This experiment is very consistent with the simulation in Section 3. For example, it is validated by comparing the visibility of the reconstructed object located at 150 mm in tangential group 1 of Figure 10. The visibility began to decrease below 0.4 when the spatial filter size exceeded 400 μm . Similarly, it is also confirmed that the object located at 150 mm could not be expressed after a size of around 400 μm through a red line of Figure 6.

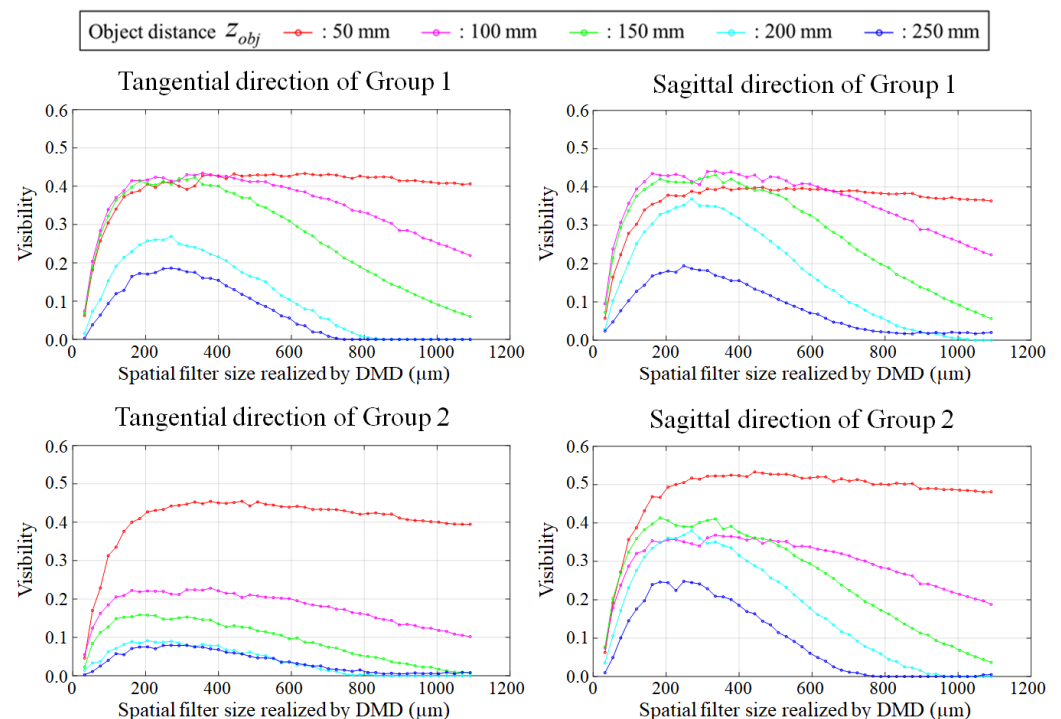


Figure 10. Visibility depending on the sagittal and tangential directions.

Consequently, the optimal spatial filter size (OSFS) was estimated to be between 200 and 400 μm . In the tangential direction of group 1, the OSFS for reconstruction at object distances of 50, 100, and 150 mm was around 350 μm because there was the highest visibility around the area. In the case of reconstructing at object distances of 200 and 250 mm, the OSFS was around 270 μm . In the tangential direction of group 2, the OSFS was considered as 400 μm when object distances were 50 and 100 mm. In the case of object distances of 150, 200, and 250 mm, the OSFS was around 200 μm . Similarly, the OSFS was obtained depending on the object distances in the sagittal direction. In group 1, in the case of object

distances of 50, 100, and 150 mm, the OSFS was around 350 μm . When object distances were 200 and 250 mm, the OSFS was 270 μm . In the case of group 2, the OSFS was around 450 μm with an object distance of 250 mm. Also, we estimated an OSFS of 300 μm at the object distances of 100, 150, and 200 mm. In case of an object distance of 250 mm, the OSFS was around 250 μm . These results indicate the OSFS differs according to object distances and it is hard to decide the OSFS. However, among the specification of a holographic display, the expressible object distance range is an important characteristic. An increase of the spatial filter size induces a narrowing of the expressible object distance range, and this is demonstrated in our experiments. Therefore, we obtained the OSFS by analyzing a figure of merit which is the negative of the sum of the measured visibilities according to the spatial filter size, r_s , and the figure of merit, M , is calculated by

$$M(r_s) = - \sum_{z_{obj}} v(r_s, z_{obj}), \quad (10)$$

where a figure of merit, M , signifies the criterion that a hologram can be accurately expressed. This indicates that the smaller the value, the better the hologram is expressed. Figure 11 shows the figure of merit, M , depending on the spatial filter size. Blue circles denote the figure of merit of the measured result corresponding to the spatial filter size, and a blue line is a regression result of the figure of merit values. Considering the tendency of visibility of Figure 10, there is no significant change between 200 μm and 400 μm in Figure 11. When the spatial filter size is 270 μm , the figure of merit, M , is the minimum value. Therefore, the OSFS is 270 μm , as indicated by the black dotted line in Figure 11.

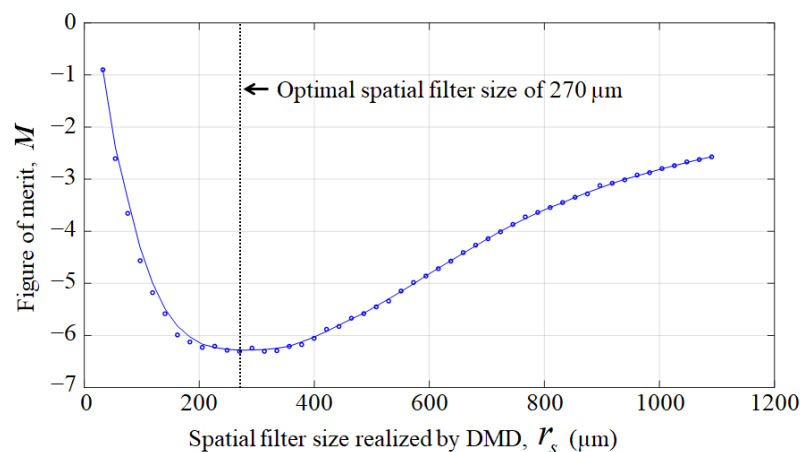


Figure 11. Optimal spatial filter size realized by DMD in experimental configuration.

Finally, we performed an experiment to reconstruct a holographic image using the LED light source with the spatial filter size of 270 μm as shown in Figure 12. Four real objects were placed at different positions from the hologram plane with the experimental setup of reconstructing the Fresnel hologram. The girl doll, rabbit doll, Rubik's cube, and the flowerpot were positioned at -500 , -200 , $+50$, and $+150$ mm from the hologram plane, respectively. For the holographic content, holograms indicating the depth of each real object were reconstructed as shown in Figure 12. The depth map CGH method was used to generate the hologram for the experiment. The reconstructed image is was while adjusting the focus with a DSLR camera. Figure 13 shows the captured images focused -500 , -200 , $+50$, and $+150$ mm from the hologram plane. These results show that the focus positions of the reconstructed hologram are equal to the positions of real objects. In addition, it is worth to noting that each reconstructed image generally appeared with good focus without the blurring.

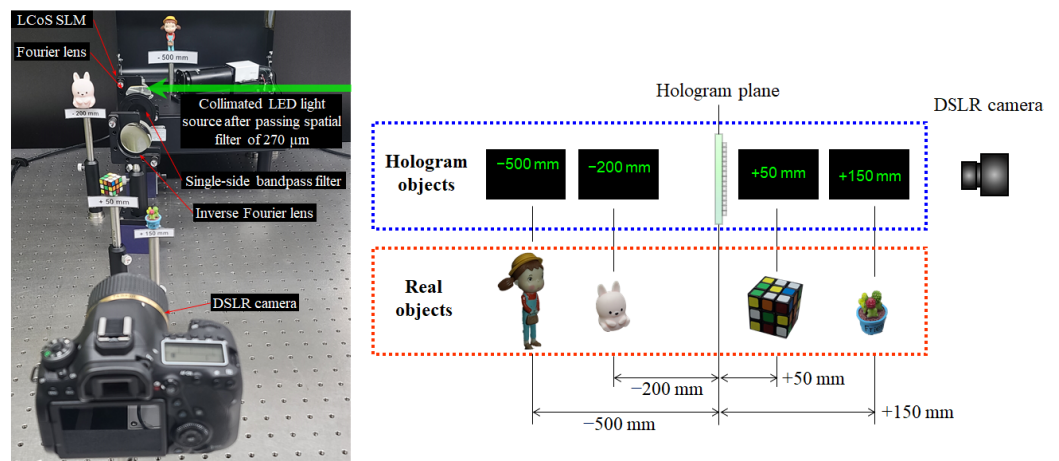


Figure 12. Experimental setup of reconstructing holographic image based on the LED light source with a spatial filter size of 270 μm .

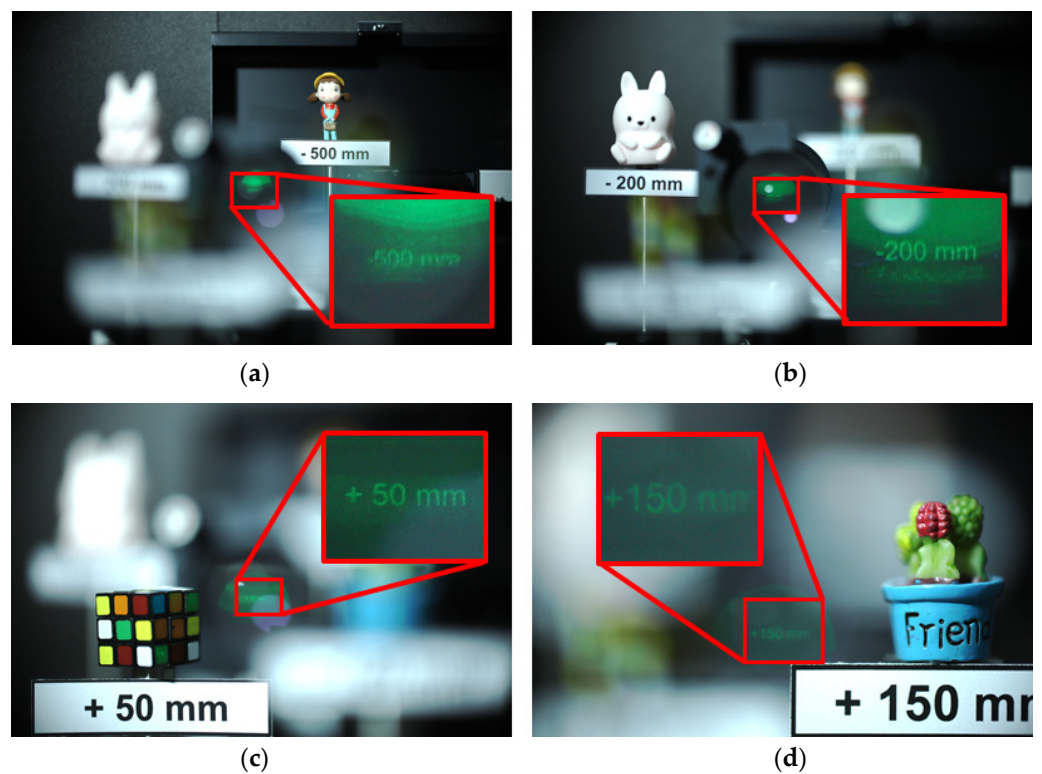


Figure 13. Reconstruction image using the LED light source with a spatial filter size 270 μm . The captured images focused at (a) -500, (b) -200, (c) +50, and (d) +150 mm from the hologram plane.

5. Discussion

We obtained an OSFS of 270 μm in our experiments, which is similar to the result of D. Chu et al. [19]. They discussed the spatial coherence of a LED light source with different emission sizes by measuring the spatial coherence value using the same double slits. Here, the spatial coherence value is equal to the visibility of the proposed analysis. From measuring the spatial coherence value by adjusting the spatial filter size from 100 μm to 1 mm per unit of 100 μm , it was shown that the theoretical tendency and experimental results are equal. They concluded that a pinhole smaller than 300 μm is sufficient to obtain a sharp holographic image, even at a short object distance. However, this is not simple, and our experimental results show that the effect of temporal coherence becomes more pronounced as the spatial filter size becomes smaller. This explains why an unconditional

decrease of the spatial filter size may adversely affect the quality of the holographic image. In our study, we analyzed the quality of holographic images by changing the spatial filter size from 32.4 to 1090.8 μm . The object distances of the holographic objects were considered in the experiment. As a result, the OSFS was obtained as 270 μm in Figure 11. In addition, we proposed an expressible object distance depending on the coherence properties of the light source, and in Section 4, it was demonstrated that our theory and experimental results are reasonable.

6. Conclusions

In this paper, a novel method for controlling the spatial coherence in a holographic display system was proposed. It was implemented to evaluate the quality change of holographic content according to the amount of the spatial coherence of the LED light source. In order to control the spatial coherence, we used a DMD as a dynamic spatial filter. The expressible object distance range, based on a geometric model of the holographic display, was calculated depending on the coherence of the light source. Both spatial and temporal coherences affected the amount of blur in the reconstructed images. By analyzing the visibility of the reconstructed hologram according to the size of the spatial filter, we obtained the optimal size of the spatial filter. When the LED light source with the central wavelength of 530 nm and FWHM of 30 nm was used, the optimal size of the light source was 270 μm . It was confirmed that the expressible object distance range in experiments was sufficiently consistent with the simulation. In the future, by inserting the temporal coherence control optics in the proposed system, we will control not only the spatial coherence but also the temporal coherence to obtain the coherence characteristics of the LED light source. It is expected that the proposed method will be helpful in determining the appropriate light source for holographic displays.

Author Contributions: Conceptualization, S.L. and J.H.; methodology, S.L. and S.A.; software, H.J.; formal analysis, S.L. and J.H.; validation, S.L. and S.A.; writing—original draft preparation, S.L.; writing—review and editing, S.L., H.J. and J.H.; supervision, J.H. All authors have read and agreed to the published version of the manuscript.

Funding: This research was funded by the Kyungpook National University Research Fund, 2021.

Institutional Review Board Statement: Not applicable.

Informed Consent Statement: Not applicable.

Data Availability Statement: Not applicable.

Conflicts of Interest: The authors declare no conflict of interest.

References

1. Gabor, D. Holography, 1848–1971. *Science* **1972**, *177*, 299–313. [[CrossRef](#)] [[PubMed](#)]
2. Hahn, J.; Kim, H.; Lim, Y.; Park, G.; Lee, B. Wide viewing angle dynamic holographic stereogram with a curved array of spatial light modulators. *Opt. Express* **2008**, *16*, 12372–12386. [[CrossRef](#)] [[PubMed](#)]
3. Lim, Y.; Hong, K.; Kim, H.; Kim, H.-E.; Chang, E.-Y.; Lee, S.; Kim, T.; Nam, J.; Choo, H.-G.; Kim, J.; et al. 360-degree table top electronic holographic display. *Opt. Express* **2016**, *24*, 24999–25009. [[CrossRef](#)] [[PubMed](#)]
4. Park, J.; Lee, K.-R.; Park, Y.-K. Ultrathin wide-angle large-area digital 3D holographic display using a non-periodic photon sieve. *Nat. Commun.* **2019**, *10*, 1304. [[CrossRef](#)] [[PubMed](#)]
5. Chang, C.; Bang, K.; Wetzstein, G.; Lee, B.; Gao, L. Toward the next-generation VR/AR optics: A review of holographic near-eye displays from a human-centric perspective. *Optica* **2020**, *7*, 1563–1578. [[CrossRef](#)] [[PubMed](#)]
6. Reynolds, G.O.; Develis, J.B. Hologram coherence effect. *IEEE Trans. Antennas Propag.* **1967**, *15*, 41–48. [[CrossRef](#)]
7. Ahn, S.; Lim, S.; Kim, M.; Hahn, J. Expressible-depth control method in digital holographic display. *Proc. SPIE* **2019**, *10944*, 109440O.
8. Lee, S.; Kim, D.; Nam, S.-W.; Lee, B.; Cho, J.; Lee, B. Light source optimization for partially coherent holographic displays with consideration of speckle contrast, resolution, and depth of field. *Sci. Rpt.* **2020**, *10*, 18832. [[CrossRef](#)] [[PubMed](#)]
9. Goodman, J.W. Some fundamental properties of speckle. *J. Opt. Soc. Am.* **1976**, *66*, 1145–1150. [[CrossRef](#)]
10. Gerritsen, H.J.; Hannan, W.J.; Ramberg, E.G. Elimination of speckle noise in holograms with redundancy. *Appl. Opt.* **1968**, *7*, 2301–2311. [[CrossRef](#)] [[PubMed](#)]

11. Lowenthal, S.; Joyeux, D. Speckle removal by a slowly moving diffuser associated with a motionless diffuser. *J. Opt. Soc. Am.* **1973**, *61*, 847–851. [[CrossRef](#)]
12. Garcia-Sucerquia, J.; Ramirez, J.A.H.; Prieto, D.V. Reduction of speckle noise in digital holography by using digital image processing. *Optik* **2005**, *117*, 44–48. [[CrossRef](#)]
13. Kang, X. An effective method for reducing speckle noise in digital holography. *Chin. Opt. Lett.* **2008**, *6*, 100–103. [[CrossRef](#)]
14. Lee, B.; Kim, D.; Lee, B.; Lee, D.; Lee, S. Speckle reduction in holographic displays. *Proc. SPIE* **2021**, *11709*, 1170906.
15. Kozacki, T.; Chipala, M. Color holographic display with white light LED source and single phase only SLM. *Opt. Express* **2016**, *24*, 2189–2199. [[CrossRef](#)] [[PubMed](#)]
16. Moon, E.; Kim, M.; Roh, J.; Kim, H.; Hahn, J. Holographic head-mounted display with RGB light emitting diode light source. *Opt. Express* **2014**, *22*, 6526–6534. [[CrossRef](#)] [[PubMed](#)]
17. Lee, D.; Lee, B. Comparison between LED and LD as a light source for near-eye holographic display. *Proc. SPIE* **2018**, *10834*, 1083419.
18. Peng, Y.; Choi, S.; Kim, J.; Wetzstein, G. Speckle-free holography with partially coherence light sources and camera-in-the-loop calibration. *Sci. Adv.* **2021**, *7*, eabg5040. [[CrossRef](#)] [[PubMed](#)]
19. Deng, Y.; Chu, D. Coherence properties of different light sources and their effect on the image sharpness and speckle of holographic displays. *Sci. Rpt.* **2017**, *7*, 5893. [[CrossRef](#)]
20. Hecht, E. *Optics*, 5th ed.; Pearson Education India: London, UK, 2002; pp. 398–456.